JOURNAL OF CATALYSIS 66, 301–315 (1980)

Morphology and Redispersion of Ir on SiO_2 in Oxidizing and Reducing Atmospheres[1]

T. WANG AND L. D. SCHMIDT

Department of Chemical Engineering and Materials Science, University of Minnesota, Minneapolis, Minnesota 55455

Received March 21, 1980; revised June 26, 1980

Structures and phases produced by heating 20- to 100-Å-diameter particles of Ir on amorphous SiO_2 in air or H_2 at a pressure of 1 atmosphere are examined by electron microscopy. The oxide is first observed to form at ~300°C, and by 700°C substantial amounts of oxide form around metal particles and spread as a thin layer over the SiO_2. At 750°C the residual metal particles are observed to break up into clusters of several smaller 10–30 Å particles. Oxidation is complete only at ~900°C. Oxide forms as a very thin layer which appears to have a lower volatility than that measured for bulk IrO_2. When small particles formed by heating in air to 750°C are subsequently heated in H_2, all oxide is reduced by 400°C to form clusters of small Ir particles. These remain stable to ~600°C, above which sintering to larger particles occurs. An oxidation–reduction cycle thus is capable of causing redispersion of Ir into smaller particles. This apparently occurs through a surface transport path, while redispersion in more mobile metals can occur only by vapor transport.

INTRODUCTION

Iridium is one of the highest melting of the Group VIII metal catalysts. Consequently, it may be expected to exhibit low sintering rates and to be less easily oxidized or reduced than the other platinum metals. Iridium forms a very stable solid oxide, IrO_2 (decomposition temperature of 1120°C in air at 1 atmosphere), but it also forms a gaseous oxide, IrO_3, whose volatility severely limits the use of Ir as a catalyst, especially in oxidizing atmospheres. Thus, Ir has the lowest metal mobility, the most stable solid oxide, and the most volatile oxide of any of the fcc Group VIII metals. It is therefore of interest to see how these properties affect the sintering and morphology of Ir crystallites.

We have recently examined the morphologies of 10 to 200 Å Pt (*1*), Pt–Pd (*2*), and Pt–Rh (*3*) crystallites on amorphous SiO_2 in oxidizing and reducing atmospheres using scanning transmission electron microscopy (STEM). Pd is readily oxidized to PdO upon heating in air at 1 atm at 300°C, and the oxide is reduced by exposure to H_2 at room temperature. Rh oxidizes to Rh_2O_3 at 600°C. From a Pt alloy PdO nucleates and grows at the side of metal particle while Rh_2O_3 forms as a skin over the metal particle; these differences can be explained in terms of the higher mobility of Pd and PdO compared to Rh and Rh_2O_3.

There has been considerable work (*4–11*) on the activity and selectivity of supported Ir and Pt–Ir catalysts, mostly on Al_2O_3, in hydrocarbon reactions, although much less has been done on sintering and morphology. Sinfelt and Via (*12*) recently investigated a series of supported Pt–Ir alloys on Al_2O_3 by H_2 chemisorption and x-ray diffraction. They concluded that Pt–Ir formed bimetallic clusters if prepared by impregnation of salts with oxidation and reduction below 500°C. However, IrO_2 formed if alloys were heated above 500°C in air. Fiedorow *et al.* (*13*) compared the sintering rates of Pt, Ir, and Rh supported on alumina in oxygen and hydrogen atmospheres. They found that the thermal stability in oxygen is Rh > Pt > Ir while in hy-

[1] This work partially supported by PRF Under Grant No. 10864-AC7.

0021-9517/80/120301-15$02.00/0

drogen it is Ir > Rh > Pt. McVicker *et al.* (*14*) proposed the idea of a "chemical trap" to explain the additional stability of Ir on Al_2O_3 in the presence of CaO, SrO, and BaO when heated in air. These investigations give a partial description of sintering of supported Ir catalysts in oxygen and hydrogen. However, the overall picture of changes in morphology under different atmospheres remains unclear.

EXPERIMENTAL

Apparatus and procedures were similar to those described previously (*1–3*). Particles between 10 and 100 Å in diameter were prepared by heating thin films of Ir on 500-Å films of amorphous SiO_2 in air, N_2, or H_2 atmospheres at temperatures up to 1000°C.

Silica substrates were prepared in these experiments by vacuum depositing Si on NaCl, floating off films in H_2O, and mounting them over small holes ion milled in 3-mm-diameter Si discs. The films and the surfaces of the discs were then oxidized by heating in air at 1200°C. This produces amorphous Si films ~500 Å thick as shown by TEM diffraction patterns. Ir films between 5 and 15 Å in thickness were then prepared by either vacuum deposition of Ir wire in a heated W wire basket or impregnation with an aqueous solution of $IrCl_3$. Film thicknesses and metal loading, determined by Ir weight loss from the basket or from the amount of Ir in a liquid drop, are believed to be accurate to within ±10%.

Specimens were heated in a 3-cm-diameter quartz tube in flowing gases at a nominal velocity of 0.5 cm^3/sec, typically for 1 hr. They were then examined by bright and dark field imaging and electron diffraction in a JEOL 100CX STEM. Samples were transferred repeatedly between the microscope and the oven; the same region was examined repeatedly by identifying characteristic regions at the edge of the hole. This arrangement and procedure were used to minimize contamination. The substrate and specimen mount were SiO_2 to eliminate contamination from support grids, and specimens were never exposed to liquids after preparation. The W basket was flashed above the Ir deposition temperature before loading with Ir wire to remove volatile impurities, and in some experiments the specimen collected only an intermediate fraction of the evaporated metal. Morphologies of Ir prepared by vacuum and $IrCl_3$ deposition appeared identical. X-Ray fluorescent microanalysis of several samples in the STEM revealed only Si and Ir. X-Ray photoelectron spectroscopy indicated traces of W and Au from a vacuum-deposited specimen although peak heights were much less than that of Ir. Experiments were carried out on approximately 10 different specimens. All observations were consistent with those described below.

RESULTS

Sintering of Films

When a 10-Å-thick film was heated in air up to 800°C, no particles were observed with diameters greater than 5 Å, and only weak diffraction patterns of IrO_2 were noted. This indicates that the Ir film oxidizes to IrO_2 which does not sinter into crystallites but remains continuous, much as was noted with Rh (*3*).

Particles of Ir were formed by heating mental films in H_2, N_2, or H_2–N_2 mixtures. Typically, crystallites 20 Å in diameter were observed after heating to 500°C, and 100-Å particles were produced by heating to 750°C. Although no attempts were made to follow sintering quantitatively for Ir, temperatures were much higher than those required for Pt, Pd, or Rh with the order of sintering of the metals under reducing conditions being Pd > Pt > Rh > Ir.

A typical micrograph of Ir crystallites produced by heating a 10-Å film in an N_2–H_2 mixture to 750°C is shown in Fig. 1a. The electron diffraction pattern, shown in Fig. 4d, indicates no crystalline phases except fcc Ir metal. Particles generally have the same shape and appearance as did Pt,

Pd, and Rh with many showing the sixfold symmetry of polyhedra exposing predominantly (111) crystal planes and some exhibiting single or multiple twins. Micrographs of Ir also showed some low contrast darker regions in addition to metal crystallites. We suspect that these may be small amounts of IrO_2 formed upon initial exposure of the Ir film to air at room temperature as described in the next section, although no diffraction lines were noted under these conditions except those of fcc metal.

No particles exhibited the "dumbbell" shapes and no particles were observed to move upon heating as would be expected if sintering occurred by particle coalescence. We believe therefore that the sole mechanism of sintering under reducing conditions is atomic diffusion rather than particle migration, just as was noted for the other metals on SiO_2 (*1–3*).

Heating in Air

The specimen shown in Fig. 1a was then heated subsequently in air at temperatures of 300, 400, 500, 550, 600, 700, and 750°C, each for 1 hr as shown in Figs. 1b–h. Weak diffraction rings of tetragonal IrO_2 are first observed at 300°C, and these increase in intensity as heating temperature increases. Between 300 and 500°C progressive increase in size of lower contrast oxide regions is noted at the edge of most particles, but metal particles roughly retain their original shape. However, the diffraction pattern of fcc Ir metal is clearly evident.

In some instances two or more adjacent metal particles were observed to move closer together upon heating in air. This is illustrated in Fig. 1b where the clusters of four, two, and three particles labeled A, B, and C, respectively, are pulled together upon heating in air to 300°C. However, heating up to 700°C produced little further motion of these or other particles. This phenomenon was not noted for Pt, Pd, or Rh. We have no detailed explanation for this low-temperature motion. It was observed on all specimens and is apparently associated with an attractive interaction between particles upon formation of an oxide "bridge" between them.

Figure 1 shows that between 300 and 500°C the main changes are the appearance of one or more regions of low contrast at the side of most particles. Between 500 and 700°C progressive oxidation of all particles occurs, and the oxide regions appear to spread over the SiO_2 as temperature is increased. However, most particles retain well-defined high contrast cores of Ir up to 700°C, and diffraction rings of metal and oxide have comparable intensities (Fig. 4e).

Further heating of this sample caused a dramatic change in morphology. At 700°C oxide spreads significantly over the SiO_2 and the cores of Ir become less distinct. At 750°C this is observed as a breakup of the cores into several smaller (typically 20 Å diameter) particles within the lower contrast oxide particle.

The identities of low and high contrast regions as IrO_2 and Ir were confirmed by dark field imaging. Figures 2a and b show bright field and dark field oxide micrographs ({101} diffraction) of specimen heated to 750°C. Only those oxide particles satisfying diffraction conditions for the circular aperture used are bright, but the relatively large low-contrast regions coincide with IrO_2. Figures 2c and d show bright and dark field ({200} diffraction) images of metal. The Ir clearly coincides with small high-contrast particles.

Histograms of the number of particles versus diameter are shown in Fig. 3a following heating to 750°C in an N_2–H_2 mixture (from Fig. 1a), to 600°C in air (from Fig. 1f), and to 750°C in air (from Fig. 1h). These were obtained by measuring diameters of ~1000 particles, and diameters shown represent the *overall diameter* of the entire particle rather than those of small metal particles in each large particle. The histograms and micrographs show that diameters of particles increase from 97 to 143 Å upon heating in air to 750°C. Since particles all grow with little sintering (mi-

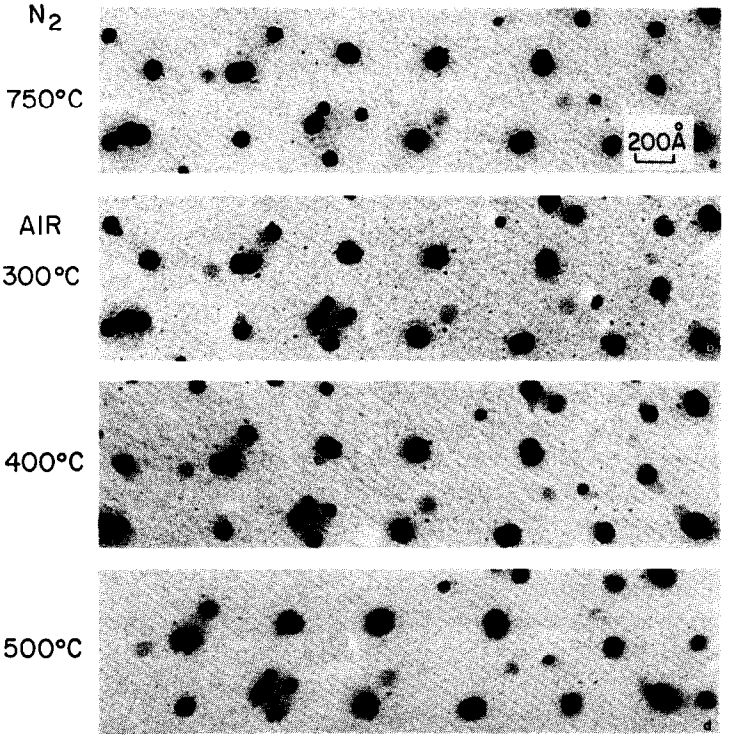

FIG. 1. Micrographs of the same Ir particles on SiO_2 following heat treated in air for 1 hr at temperatures indicated. The 97 Å average diameter particles were prepared initially in (a) by heating in an N_2–H_2 mixture to 750°C. Oxide is evident at 300°C and the amount increases to 600°C. At 700 and 750°C metal cores break up into very small particles.

gration of Ir from one particle to another) and some Ir may have evaporated as IrO_3, this places a bound on the decrease in particle height or thickness of ~2.2 upon treatment in air. Alternately, the height to diameter ratio decreases by a factor of 3.4 upon oxidation to this stage.

Complete Oxidation of Ir

Another sample, shown in Fig. 4, with approximately the same loading of Ir as in Fig. 1 was heated following the same procedures as before. However, this sample was heated up to 800 and 900°C successively for 1 hr in order to oxidize the small Ir particles completely to IrO_2. Figures 4a, b, and c show micrographs of this sample after heat treatments at 750, 800, and 900°C, respectively. These specimens exhibit very low contrast, and the micrographs shown in this figure were taken by using the smallest objective aperture available in order to maximize contrast. These micrographs show that complete oxidation occurred between 800 and 900°C, and oxide particles continue to spread over the substrate at these temperatures. The electron diffraction pattern of the specimen shown in Fig. 4c is shown in Fig. 4f. Only the lines of IrO_2 are detected.

Iridium Vaporization

Iridium readily vaporizes as IrO_3 when heated in oxygen as indicated by the weight loss experiments of Krier and Jaffee (*15*) measured between 1000 and 1400°C. Their extrapolated results indicate that the evaporation rate of IrO_3 is 0.5 mg/cm²-hr at 900°C in air at 1 atmosphere, and therefore no Ir or IrO_2 should remain on the surface in these experiments. To confirm the Krier and Jaffee results and extend them to the

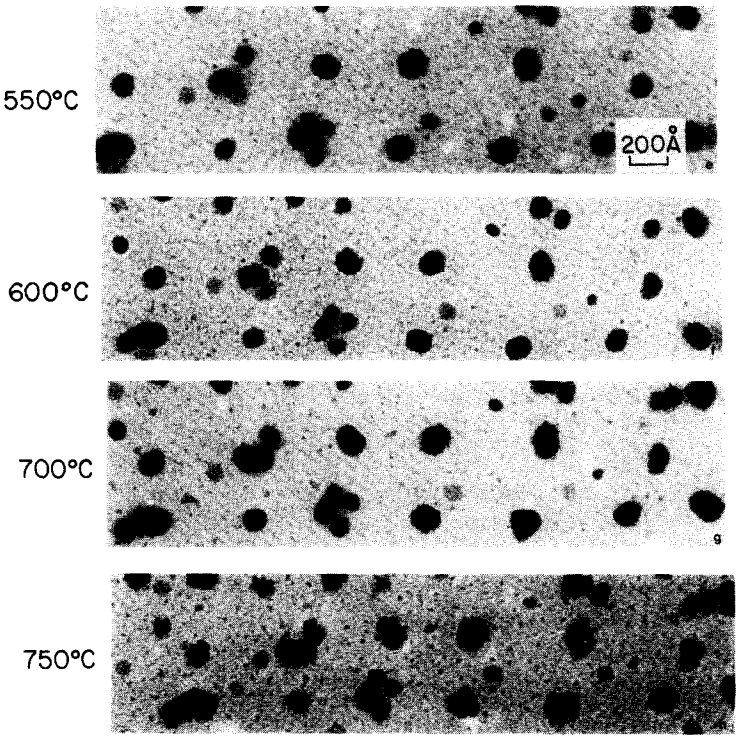

FIG. 1—*Continued.*

temperature of these experiments, we measured the rate of weight loss of an Ir wire in the same tube used for particle heating. Figure 5 shows the rate of metal loss measured at temperature between 650 and 750°C. As will be discussed later, these rates should not fall on the same Arrhenius plot as those of Krier and Jaffee because different solid phases are present.

However, it is clear from these measurements that IrO_2 is present on the SiO_2 at temperatures far above those where volatilization should occur.

Oxidation of Smaller Ir Particles

All results described have been on particles sintered to an average initial diameter of ~100 Å. In Fig. 6a is shown micrograph particles prepared by heating at 500°C in H_2 for 1 hr. This treatment produces a bimodal size distribution with most particles ~10–20 Å in diameter and some particles 40–60 Å in diameter. This behavior was confined on several specimens by comparable treatment. A similar result was reported by Baker *et al.* (*14*) who showed a micrograph in which large particles are visible and the presence of smaller particles was reported.

Figures 6b and c show micrographs of the same sample after heating in air to 600 and 750°C, respectively. Particles have sintered in Fig. 6b and some large (100–200 Å diameter) low-contrast regions of oxide have formed. Upon heating to 750°C oxide regions grow and increase in density, small particles sinter significantly, and some regions appear to be free of particles.

For these small particles oxide appears to nucleate and grow only in certain regions. We suggest that the bimodal size distribution may be associated with oxide which forms on the film after preparation and beore heating in H_2.

However, we have no detailed explanation for either the bimodal distribution, the

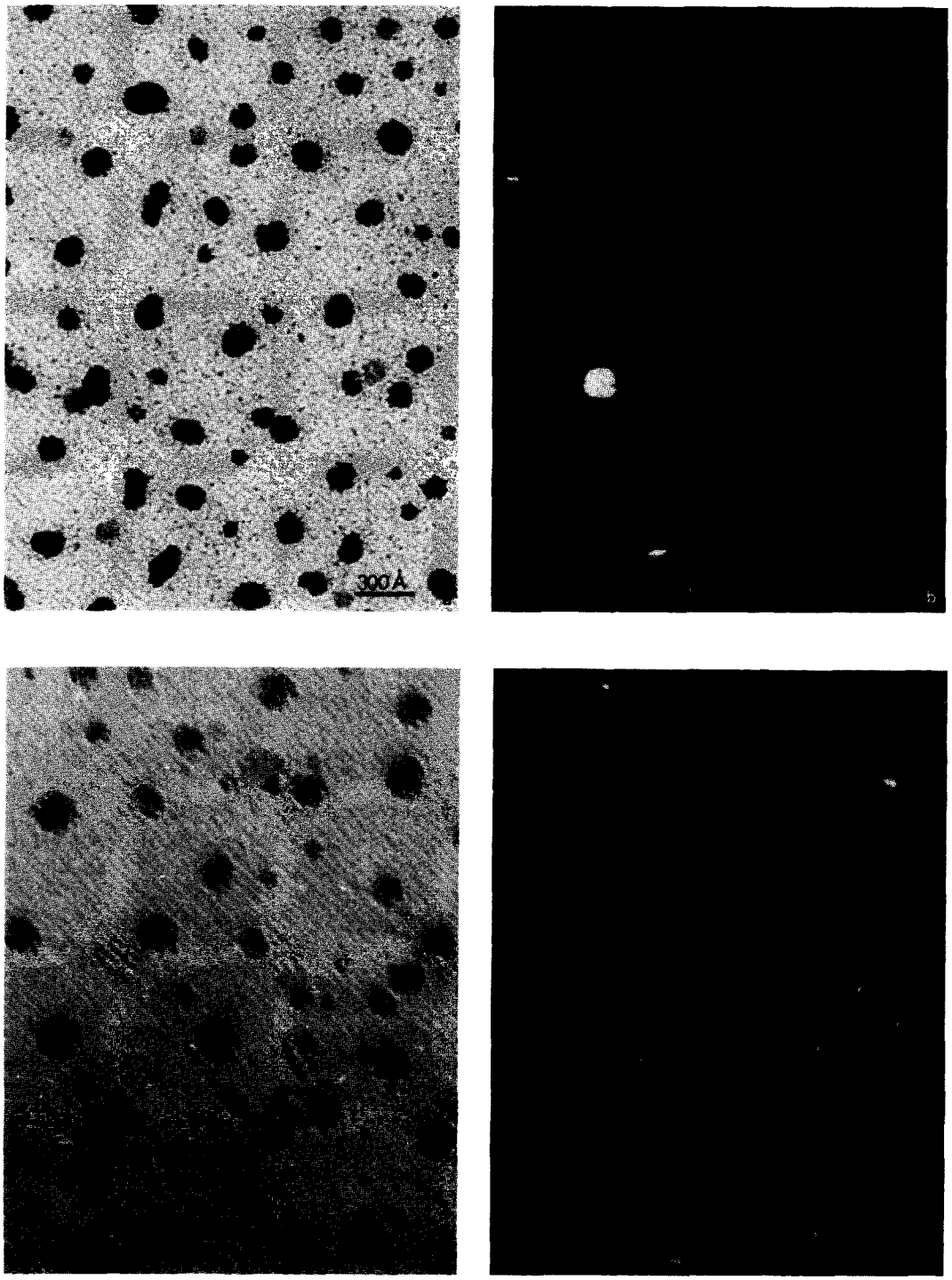

FIG. 2. Dark field micrographs showing IrO_2 (b) and Ir metal (d) for bright field micrographs of (a) and (c), respectively, following heating in air at 750°C to form small Ir metal particles within original oxide particle. The low-contrast region corresponds to large IrO_2 crystals while small particles are Ir metal.

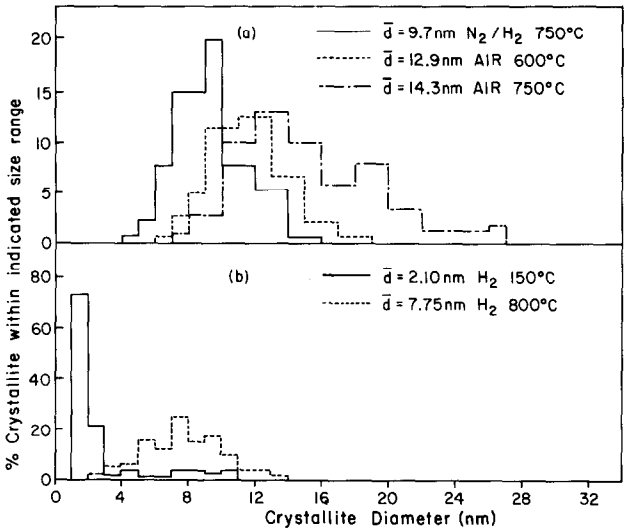

FIG. 3. (a) Number versus diameter histograms showing initial Ir particles heated in an N_2–H_2 mixture at 750°C, following heat in air at 600 and 750°C, respectively. Particles appear to increase in size upon heating at these temperatures primarily because they "spread" over the SiO_2 to form thin layers of IrO_2. (b) Number versus diameter histograms of Ir metal after heating in H_2 at 150 and 800°C, respectively.

nucleation of IrO_2, or the existence of regions apparently free of Ir. However, these experiments were repeated several times with consistent behavior as noted above.

Heating in H_2

The reduction of the same sample shown in Fig. 1 was carried out after the observations described previously. Figures 7a to h show the sequence of micrographs taken after heating in H_2 at 150, 200, 300, 400, 500, 600, 700, and 800°C, respectively. At 200°C, weak diffraction ring patterns of fcc metal could be detected. At 400°C, the diffraction pattern indicated that all oxide was reduced to metal. No obvious sintering of Ir can be observed from the temperatures between 150 and 500°C (Figs. 7a to e), but one can see "shrinking" of the particles which accompanies IrO_2 reduction to Ir.

Sintering of small (~20 Å diameter) Ir particles occurs significantly at temperatures greater than 600°C. By comparing of Figs. 7f, g, and h, one can see that many smaller Ir particles disappear and larger ones grow. However, neither particle coalescence events nor dumbbell shaped particles were observed at intermediate steps of sintering (Fig. 7g). Those particles which pulled together the intermediate island shapes and finally coalesce (Fig. 7h). Thus we conclude that atomic migration is still the dominant mode of sintering of Ir on SiO_2.

These observations were made more quantitative by measuring number versus diameter histograms of Ir particles heated in H_2. Figure 3b shows histograms from Figs. 7a and h, respectively, while Fig. 8 shows average diameter versus temperature from micrographs of Fig. 7. The average diameter remains unchanged to ~600°C (particles are unaffected by heating), but the average diameter increases from 21 to 80 Å between 600 and 800°C.

DISCUSSION

Comparison Between Pt, Pd, Rh, and Ir on SiO_2

Figure 9 summarizes the morphologies of the metals and alloys formed upon heating in H_2 or air to temperatures indicated for

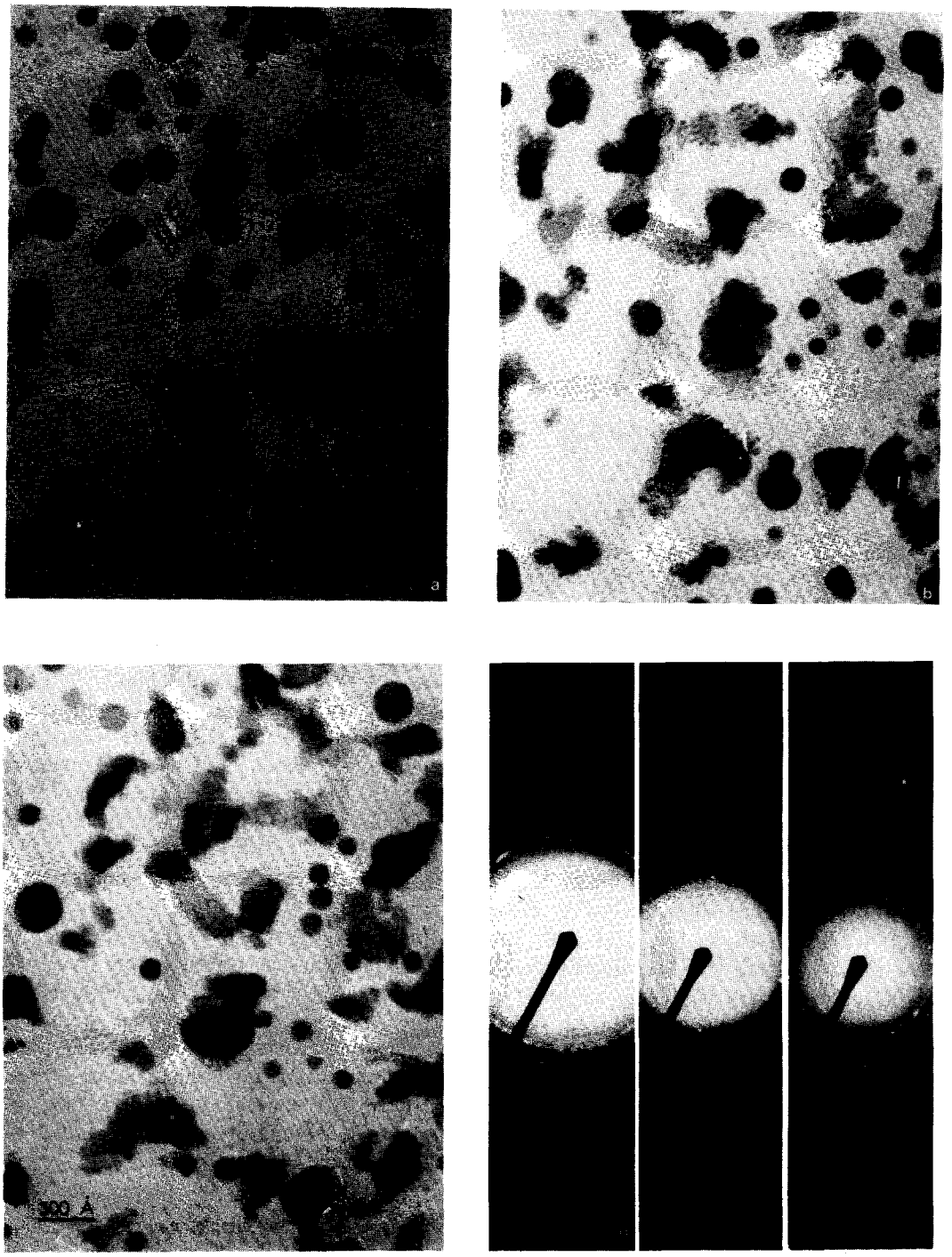

FIG. 4. Micrographs showing final stages of Ir oxidation at 750°C (a), 800°C (b), and 900°C (c), respectively. (d), (e), and (f) show electron diffraction patterns of Ir, Ir + IrO_2, and IrO_2, respectively, from specimens whose micrographs are shown in Figs. 1a, 1g, and 4c.

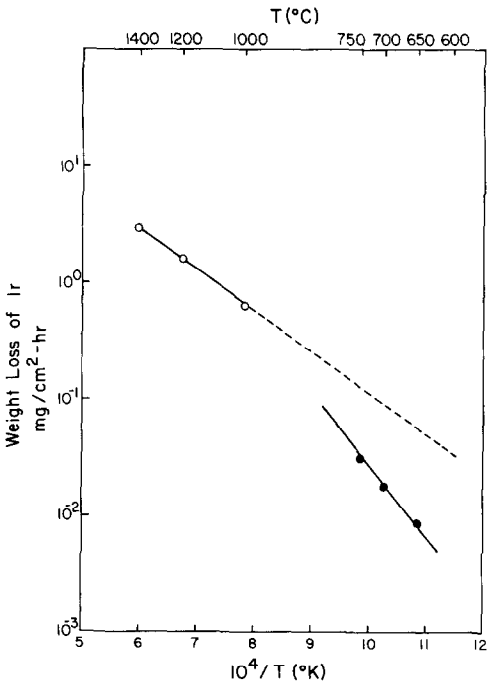

FIG. 5. Weight loss of Ir wire in flowing air at elevated temperatures. Open circles represent data from Krier and Jaffee, and solid circles represent our results.

1 hr, and Table 1 indicates the approximate temperatures required for particle formation, oxidation, reduction, and volatilization. These are estimated from our present and previous experiments for typically 1-hr heating periods at temperatures indicated.

Sintering of metals in H_2 or N_2 proceeds by atomic surface diffusion, and diffusion coefficients should correlate inversely with melting points: Ir > Rh > Pt > Pd. Table 1 shows that temperatures for particle formation are in this order. This agrees with the conclusions of Fiedorow *et al.* (*13*).

Oxidation and reduction presumably proceed by diffusion of O_2 or H_2 through metal or oxide layers, or by bulk diffusion of metal or oxide, and data in Table 1 also correlate with melting points.

Volatilization in air should correlate with vapor pressures of volatile oxides, PtO_2, PdO, Rh_2O_3, and IrO_3. These are roughly as shown in Table 1, although PdO decomposes to Pd at 750°C without significant volatilization of oxide. The apparent suppression of volatilization of IrO_3 is the only obvious anomaly between observed behavior and bulk thermodynamic properties of the metals and their oxides.

The morphologies produced in oxidation are also similar for Pd, Rh, and Ir. Oxide forms on the SiO_2, but for Pd this nucleates and grows either at the edge of the metal particle or as a separate particle. For Rh and Ir a skin of oxide first forms which then spreads over the SiO_2 at higher temperatures. These differences are also apparently correlated with mobilities of metal and oxide species.

The separation of metal oxide from the parent metal particle is presumably due to the relative interfacial energies between metal and metal oxide, between metal and SiO_2, and between metal oxide and SiO_2. Calling these surface free energies γ_{M-MOx}, γ_{M-SiO_2}, and $\gamma_{MOx-SiO_2}$, the results imply that

$$\gamma_{MOx-SiO_2} < \gamma_{M-MOx} < \gamma_{M-SiO_2}$$

for all three metals which form oxides. The dominant interaction is evidently the very strong adhesion (low interfacial tension) between metal oxides and SiO_2. However for none of these systems is this interaction strong enough to produce new compounds between metal oxide and silica.

The area on the substrate which is occupied by metal or metal oxide is increased by 65 and 108% at 600 and 750°C, respectively. The spreading of metal oxide on the oxide substrate, which implies strong interaction between support and oxide, had been observed by many investigators and summarized by Geus (*16*) and Anderson (*17*). Generally the energy of adhesion between metal and support in the absence of oxygen is in the range of 8 kcal/mole, which indicates no more than a van der Waals interaction. However, in the presence of oxygen at high temperatures (or the formation of oxide), the interaction energy may be increased to within the range of chemical bonds (*17*).

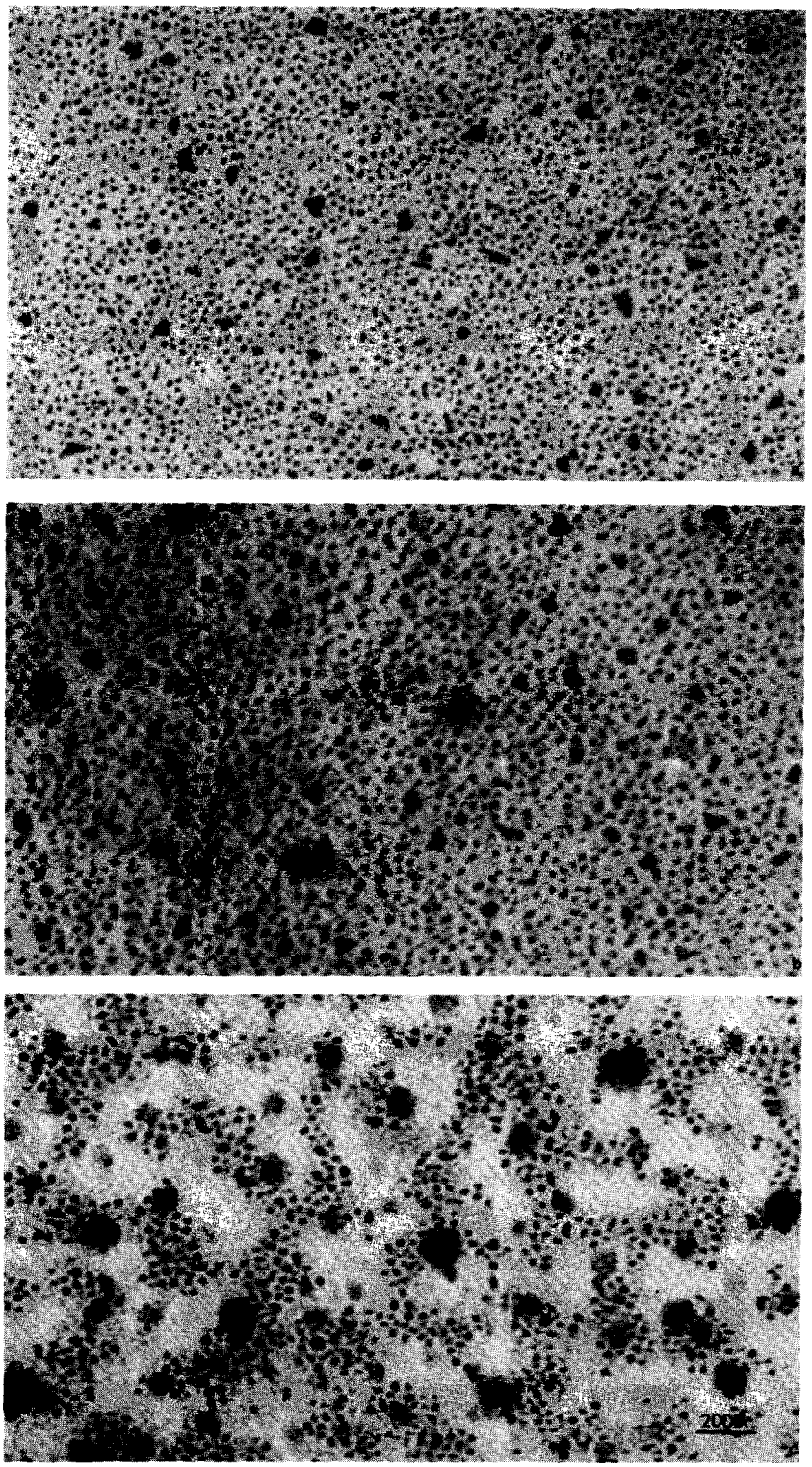

FIG. 6. Micrographs of a well-dispersed Ir on amorphous SiO_2 after heating in H_2 for 1 hr at temperatures of (a) 500°C, (b) in air at 600°C, and (c) 750°C. While many Ir particles disappeared due to sintering and evaporation, the accumulation of large IrO_2 crystallites is observed.

It is interesting to speculate on the possible cross-sectional profiles of metal, oxide, and SiO_2 when metal and oxide coexist. Figure 10 shows four possible idealized configurations. Figure 10a is the most likely structure for a *partially* oxidized Ir or Rh particle which forms at low temperatures as a skin over the metal core. Figure 10b is the structure proposed for Pt alloys with Rh and Ir. However, if the interfacial energy differences are sufficiently great, oxide could penetrate under the metal particle as shown in Figs. 10c and d.

Iridium Oxide Particles on SiO_2

The irregularly shaped particles formed by heating in air are found to be IrO_2, the stable bulk oxide. The observation of these particles coincides with the appearance of IrO_2 diffraction lines, and dark field images with these diffraction lines confirms this structure.

However two factors are not obviously consistent with this picture: (i) the oxide particles appear to be very thin and thus may not be expected to yield strong and sharp diffraction and (ii) the oxide appears to have a vapor pressure lower than that of bulk IrO_2.

The original Ir particles presumably have heights which are an appreciable fraction of their diameters, and the increase in diameter which accompanies oxidation indicates that the height-to-diameter ratio decreases significantly upon oxidation. We estimate oxide particles to have an average thickness of no more than 10 Å. This comes from assuming that all of the initial Ir film deposited remains on the surface upon oxidation and that all particles have uniform thickness. This estimate is a lower bound because some Ir evaporates as IrO_3 upon heating in air and some oxide may exist in thicker layer particles. Thickness of a crystalline particle is difficult to assess from images alone because of diffraction contrast.

There has been considerable discussion in the literature of very thin metal particles or "rafts" (*18–20*), suggested to be only a single atom layer thick from chemisorption uptake measurements. We suggest that IrO_2 may be only a few atom lyers thick, but that Ir metal appears to be definitely three dimensional.

The intensity and sharpness of IrO_2 electron diffraction appears to be a strong argument for the particles being three dimensional because, while the line broadening is determined by the crystal dimension parallel to the electron beam (and thus nearly perpendicular to the substrate), the particle must have a well-developed crystal structure to exhibit diffraction, and a monolayer or a bilayer should probably not exhibit a bulk structure. However, it should be noted that line broadening and crystal structure determination are usually described in the kinematic or single scattering formalism while electron scattering is so strong that the dynamical formalism is applicable (*21, 22*). Thus electron diffraction may sample short-range order much more than conventional kinematic diffraction theory implies.

The oxide on SiO_2 appears to exhibit an effective vapor pressure much lower than that of bulk IrO_2. Vaporization occurs through the reactions

$$IrO_2(s) + \tfrac{1}{2}\, O_2(g) \rightleftarrows IrO_3(g)$$

and

$$Ir(s) + \tfrac{3}{2}\, O_2 \rightleftarrows IrO_3(g).$$

The oxidation of Ir,

$$Ir(s) + O_2(g) \rightleftarrows IrO_2(s),$$

has a dissociation pressure of 0.2 atmospheres of O_2 at 1010°C, so in equilibrium with air at 1 atmosphere $IrO_2(s)$ should form below this temperature. Therefore above 1010°C volatilization should occur from an Ir surface, and below this temperature from $IrO_2(s)$. The results of Krier and Jaffee were presumably obtained for Ir while our low-temperature volatilization experiments were presumably from IrO_2. The activation energies measured in these experiments, 16 and 19 kcal/mole, respec-

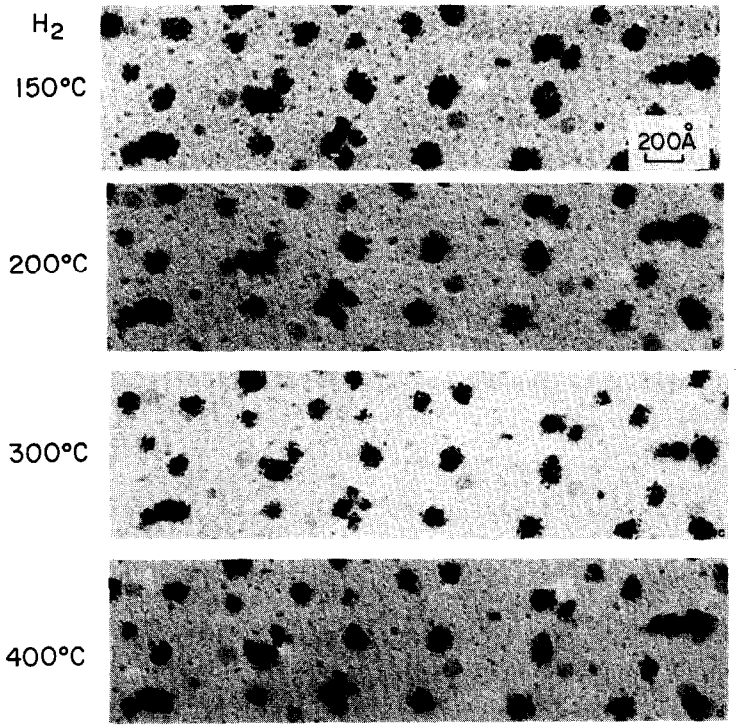

FIG. 7. Micrographs showing effects of heating partially oxidized Ir particles in H_2 at temperatures of 150, 200, 300, 400, 500, 600, 700, and 800°C. The sample is the same as that shown in the sequence of Fig. 1 and the sample had been treated in air at 750°C as shown in Fig. 1h before exposure to H_2 in Fig. 7a. All oxide is reduced at 400°C but small metal particles remain to ~700°C after which rapid sintering occurs.

tively, are different than the thermodynamic heats of vaporization, and at 4 and 58 kcal/mole, respectively (*23*), the rates of weight loss are several orders of magnitude lower than those predicted from thermodynamic equilibrium. Thus in both weight loss experiments significant mass transfer resistance must occur. We estimate that mass transfer should retard the rate of weight loss by a factor of ~1000 for the geometry and flow conditions of these experiments, and there should be little difference in rates from wires and particles on planar substrates according to these calculations.

At 900°C, thermodynamic equilibrium predicts a flux of $IrO_3(g)$ from the surface

TABLE 1

Temperatures for Transformations of 50 Å Particles on SiO_2 in H_2 and Air[a]

	Particle formation from 10 Å film (°C)	Complete oxidation (°C)	Complete reduction of oxide (°C)	Complete volatilization in air (°C)
Pt	500	—	—	800
Pd	300	400	<25	750 (decomposes)
Rh	650	550	200	>1000
Ir	750	900	400	~950

[a] Approximate temperatures in gases at 1 atmosphere for 1 hr.

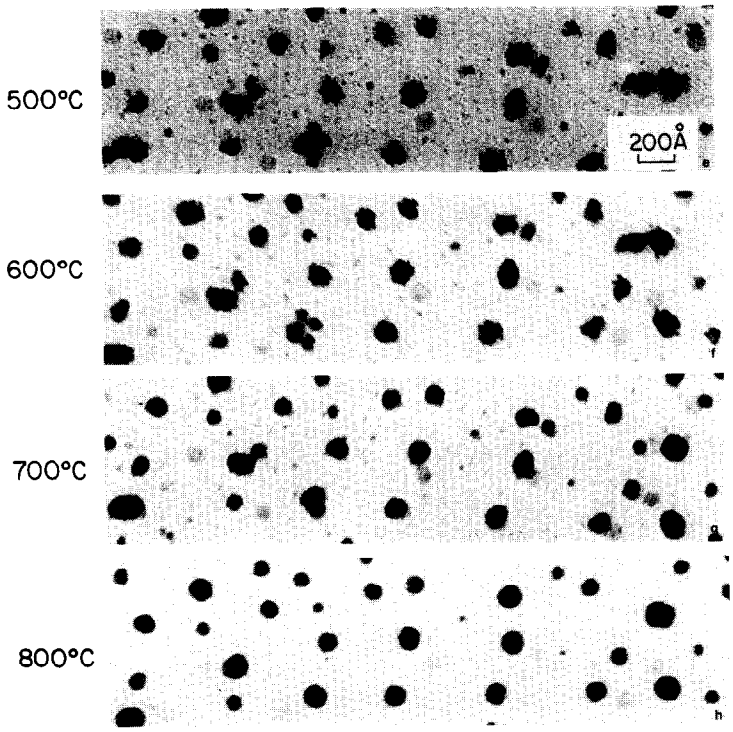

FIG. 7—*Continued.*

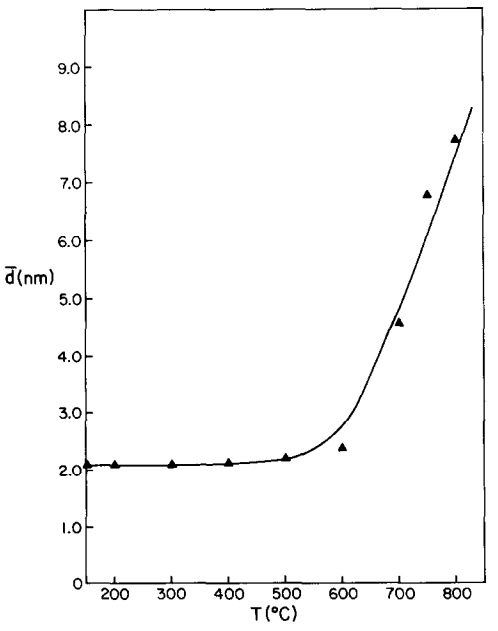

FIG. 8. Plot of average particle diameter $\bar{d}$ of Ir metal versus temperature in the reduction sequence. Notice that small Ir crystallites sinter only at temperatures above 600°C.

corresponding to 1×10^7 monolayers/sec, the wire weight loss experiments gave 1.5×10^3 monolayers/sec, and an upper bound on the rate of loss of iridium from SiO_2 gave $<10^{-3}$ monolayers/sec. Thus

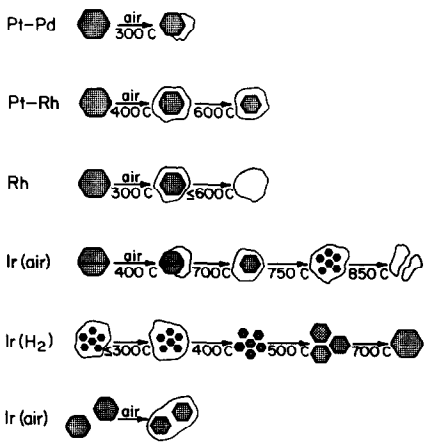

FIG. 9. Idealized sketch of observed morphologies of metals and alloys on planar SiO_2 produced by heating in H_2 or air at temperatures indicated.

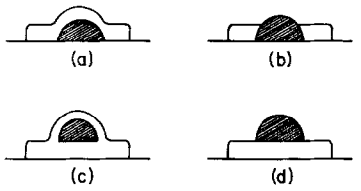

FIG. 10. Idealized sketches of possible cross-sections of metal and oxide on SiO_2.

there appears to be a significantly lower volatilization rate from small solid oxide particles on SiO_2.

It should also be noted that, if oxide volatilization is suppressed on SiO_2, the IrO_2 over an Ir particle should probably behave "normally" and evaporate at a temperature below the 900°C needed for this IrO_2 on SiO_2. This implies that the cross-section for Ir–IrO_2 would not be shown in Figs. 10a or c, but rather as 10b or d. It is interesting to speculate that the breakup of large Ir particles into tiny particles at 700–750°C may be associated with evaporation of the oxide skin covering the metal particles at lower temperatures (Figs. 10a or c). A similar morphology could also be operative in the low temperature (300°C) movement of metal particles toward each other as shown in Figs. 1a and b upon formation of a thin oxide film between them. As sketched at the bottom of Fig. 9, the presence of the IrO_2 layer between them (and presumably below particles) enables metal particles to move.

SUMMARY

Iridium particles have the lowest oxidation and reduction rates of any of the four metals studied on SiO_2 in this laboratory. Relative rates appear to be correlated with mobilities of the metals as expected if transformations are limited by metal or oxide bulk or surface diffusion. Iridium oxide forms as thin particles as do PdO and Rh_2O_3. This is consistent with a strong adhesion of the oxide with SiO_2 compared with that between metal and metal oxides. However the IrO_2 particles exhibit a suppressed vapor pressure even though they produce diffraction patterns of bulk IrO_2. This suggests that the crystal structure of bulk IrO_2 is developed for crystals smaller than is required for bulk thermodynamic properties to apply.

Redispersion of Ir produced by oxidation–reduction cycling apparently occurs by a breakup of a metal particle at ~750°C in air and nucleation of oxide into small Ir particles upon reduction. We have no satisfactory explanation for the mechanism of this process, but it provides a clear demonstration of redispersion by processes involving only solid species.

REFERENCES

1. Chen, M., and Schmidt, L. D., *J. Catal.* **55**, 308 (1978).
2. Chen, M., and Schmidt, L. D., *J. Catal.* **56**, 198 (1979).
3. Chen, M., Wang, T., and Schmidt, L. D., *J. Catal.* **60**, 356 (1979).
4. Foger, K., and Anderson, J. R., *J. Catal.* **59**, 325 (1979).
5. Rasser, J. C., "Platinum-Iridium Reforming Catalysts." Delft University Press, Delft, 1977.
6. Rasser, J. C., Beindorft, W. H., and Scholten, J. J. F., *J. Catal.* **59**, 221 (1979).
7. Plunkett, T. J., and Clarke, J. K. A., *J. Catal.* **35**, 330 (1974).
8. Karpinski, Z., and Clarke, J. K. A., *J. Chem. Soc. Faraday Trans. I* **71**, 2310 (1975).
9. Boudart, M., and Ptak, L. D., *J. Catal.* **16**, 90 (1970).
10. Sinfelt, J. H., *Catal. Rev.* **3**, 175 (1969).
11. Anderson, J. R., and Avery, N. R., *J. Catal.* **5**, 446 (1966).
12. Sinfelt, J. H., and Via, G. H., *J. Catal.* **56**, 1 (1979).
13. Fiedorow, R. M. J., Chahar, B. S., and Wanke, S. E., *J. Catal.* **51**, 193 (1978).
14. McVicker, G. B., Garten, R. L., and Barker, R. T. K., *J. Catal.* **54**, 14 (1978).
15. Krier, C. A., and Jaffee, R. I., *J. Less Common Metals* **5**, 411 (1963).
16. Geus, J. W., *Material Sci. Res.* **10**, 29 (1975).
17. Anderson, J. R., "Structure of Metallic Catalysts," p. 275. Academic Press, New York, 1975.
18. Yates, D. J. C., and Sinfelt, J. H., *J. Catal.* **8**, 348 (1967).

19. Sinfelt, J. H., *J. Catal.* **29,** 308 (1973).
20. Prestridge, E. B., Via, G. H., and Sinfelt, J. H., *J. Catal.* **50,** 115 (1977).
21. Cowley, J. M., "Diffraction Physics." American Elsevier, 1975.
22. Yacamán, M. J., and Ocana, T., *Phys. Status Solids* (*a*) **42,** 571 (1977).
23. Brain, I., Knacke, O., and Kubaschewski, O., "Thermochemical Properties of Inorganic Substances." Springer-Verlag, New York, 1977.